Manuscript accepted in Environmental Science & Technology doi: 10.1021/acs.est.0c00706

Quantifying the impact of anthropogenic atmospheric nitrogen deposition on the generation of hypoxia under future emission scenarios in Chinese coastal waters

Yu Yan YAU[1], David M BAKER[2] & Benoit THIBODEAU[1]*

[1] Department of Earth Sciences and Swire Institute of Marine Science, The University of Hong Kong

[2] School of Biological Sciences and Swire Institute of Marine Science, The University of Hong Kong

*Corresponding author: bthib@hku.hk

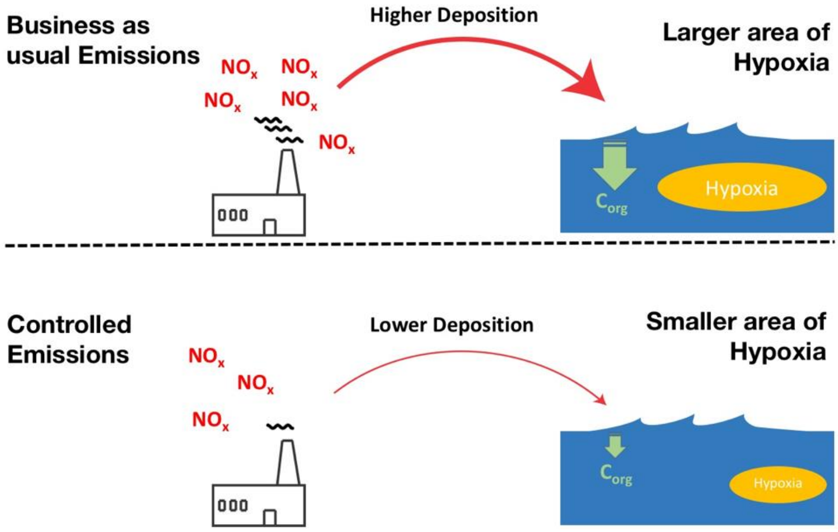

Business as usual Emissions
NOx
NOx
NOx
NOx
NOx
Higher Deposition
Larger area of Hypoxia
Corg
Hypoxia
Controlled Emissions
NOx
NOx
NOx
Lower Deposition
Smaller area of Hypoxia
Corg
Hypoxia

TOC ART

Abstract

Atmospheric deposition is an important source of nitrogen to coastal waters. In nitrogen-limited waters, the atmosphere can contribute significantly to eutrophication and hypoxia. This is especially true in China, where nitrogen emissions have increased dramatically and are projected to further increase in the future. Here, we modelled the potential future impact of change in atmospheric nitrogen deposition on hypoxia in Chinese coastal seas. We used changes in nitrogen deposition under two IPCC scenarios that included emission regulation and climate change (representative concentration pathways RCP 4.5 and 8.5) to evaluate the impacts of such deposition on hypoxia in the 2030s and 2100s. We found that, by 2030, the extent of hypoxic areas would increase up to 5% in China seas under RCP 8.5 due to the projected increase in nitrogen deposition. However, hypoxia extent was projected to decrease by up to 9% by 2100 once emission regulations included in RCP 4.5 and 8.5 are implemented. The South China Sea was found to be the most sensitive region to changes in nitrogen loads, which indicates that more effort in emissions control is needed in order to avoid expansion of the hypoxic zones in that specific region.

Introduction

Humans have significantly altered the cycling of atmospheric nitrogen (N) since the industrial revolution.[1–3] Over the past decades, industrial and agricultural advancements in addition to urbanisation have contributed to a rapid increase of N production. Nitrogen is often the limiting nutrient controlling productivity in aquatic environments;[4–6] therefore, excess N can directly impact the biogeochemical cycling in lakes, coastal regions and even the open ocean.[7–12] Eutrophication and hypoxia are usually triggered by excessive nutrients. Many studies have identified that hypoxia is associated with anthropogenic activities, such as industrial and agricultural practices, which promote enhanced nutrient delivery via rivers and waste discharge.[13] These phenomena may provide additional dissolved inorganic nitrogen to coastal regions, triggering the growth of phytoplankton and increasing oxygen consumption.

Atmospheric deposition is a non-negligible source of N to coastal waters. Elevated anthropogenic N emissions sourced from fossil fuel combustion and fertilizer use increases N deposition to the ocean.[14,15] The atmospheric N deposition supports up to 3% of annual new marine biological production globally.[16–18] China is one of the hotspots for N deposition, which has increased dramatically from 13.2 kg ha^{-1} yr^{-1} to 21.1 kg ha^{-1} yr^{-1} from 1980 to the 2000s[16,19]. Evidence shows that this elevated N could lead to environmental problems such as eutrophication and hypoxia.[20]

Atmospheric N deposition in N-limited aquatic systems can trigger the growth of phytoplankton and zooplankton.[3,7,16,21–23] Marine organic matter produced from their growth sinks to bottom waters and accumulates in sediments, where it is decomposed by bacteria, consuming dissolved oxygen in the process.[24–26] The high demand of oxygen consumption from microbial respiration and nitrification can thus decrease the concentration of dissolved oxygen in poorly-ventilated bottom waters and thereby lead to hypoxia.[25,27,28] Moreover, N in organic matter is remineralized and can be returned as new inorganic nutrients to the euphotic zone by vertical mixing and upwelling, producing the so-called N cascade (Figure 1).[16,29–31] Increases in ocean productivity can thus lead to the expansion of hypoxic zones, often called dead zones, which are frequently observed in the Gulf of Mexico, Chesapeake Bay, the St. Lawrence Estuary, the Baltic Sea and many other coastal ecosystems.[32–37] Hypoxic areas are usually located near productive fisheries crucial to the economy of adjacent communities and multiple stakeholders, such as in the case of the Gulf of Mexico.[35] Fish death due to hypoxia can therefore cause considerable economic losses.[38–41] As such, increases in atmospheric N deposition may induce a cascade of ecological, economic and social consequences.[22,31,42,43]

Eutrophication and seasonal hypoxia have been major environmental issues in China.[44–48] During the summer of 2006, a hypoxic zone of more than 15,000 km^2 was reported in the East China Sea near the Yangtze River.[49,50] The East China Sea is one of the largest coastal oxygen-depleted regions globally, and is simultaneously a major Chinese fishery.[50,51] Although river and groundwater discharge contributes to the high nutrient input to coastal waters in China,[52] atmospheric deposition also plays a key role in supplying N (Figure 1).[53–56] Due to industrialization, increased use of vehicles and food production[57], China is one of the largest emitters of anthropogenic N globally.[58] Anthropogenic N emissions in China increased 6-fold from the 1980s to 2010s, and are predicted to increase until 2030.[59] This rapid increase of N emissions on land causes a large increase of atmospheric N deposition on both land and in the surrounding ocean.[54,60–67] The deposition of this emitted N rose by 60% from 1980 to 2000 in China.[68] Despite increased emission and deposition of N in Asia, the northwestern Pacific ocean and the east part of the Sea of Japan is predicted to remain N-limited.[69] Although the Pearl River and Yangtze River are rich in nitrogen, beyond the plume area of South China Sea, East China Sea and Yellow Sea have a relatively low N:P ratio[70–73]. Hence, increases in atmospheric N deposition are likely to directly affect the primary productivity and nutrient cycling in the South China Sea and the other regions considered here.

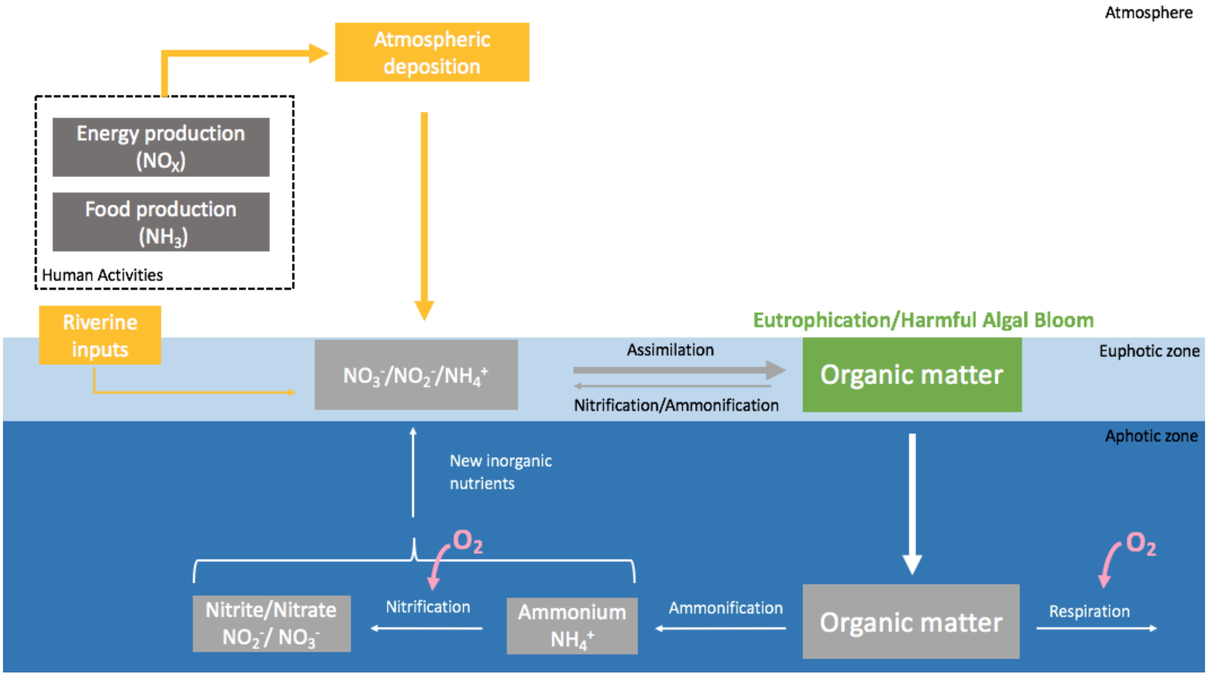

Figure 1. Schematic graph of the contribution of atmospheric deposition to hypoxia in the coastal marine environment. The atmosphere receives N from combustion of fossil fuels and the use of fertilizers. Because of the relative short residential time in the atmosphere, N can directly be deposited to the coastal ocean. Consequently, additional nutrients in the surface ocean may stimulate the rapid production of organic matter in N-limited coastal oceans and thus enhance primary productivity. Thus, this addition of N can increase the risk and duration of harmful algal blooms. When organic matter sinks to bottom waters, oxygen is consumed by different pathways such as respiration, degradation of organic matter and nitrification. When oxygen consumption exceeds oxygen supply in the water column, hypoxia is generated.

Climate change can influence hypoxia through various mechanisms. A warmer climate may stratify the water column, which inhibits the vertical exchange of oxygen and thus the replenishment of oxygen.[74] Higher temperatures also reduce the solubility of oxygen in seawater and increases microbial activity, supporting enhanced degradation of organic matter in bottom waters and thus contributing to increased oxygen demand.[28,75,76] Changes in precipitation will also affect the amount of N deposited, since precipitation is one of the main factors controlling the wet NOy deposition.[77,78] Precipitation is predicted to increase in eastern south China,[79,80] and therefore could be an additional mechanism for enhancing atmospheric nitrogen deposition and increasing hypoxia. In addition to China, this effect may also be particularly significant throughout India and Southeast Asia[81]. Hence, it is crucial to understand how climate change and anthropogenic emissions manifest changes in N deposition, and its particular impact on Chinese coastal waters. While various studies have estimated atmospheric N deposition over continental China.[82,83] and its implications for primary productivity in Chinese coastal seas,[54,84] the indirect biogeochemical consequences of atmospheric deposition such as the generation of hypoxia are seldom included. Moreover, it is difficult to isolate the effect of a single source of nitrogen when analysing field data. Thus, the impact of deposited N on hypoxia in China coastal waters is still unresolved and unquantified.

Here, we quantified the future impact of changes in N deposition on the extent of hypoxic areas in Chinese coastal waters using the future changes in atmospheric deposition over coastal China under the impact of climate change and emissions scenarios. We used the projection results from the Atmospheric Chemistry and Climate Model Intercomparison Project (ACCMIP), which accounts for the Representative Concentration Pathways (RCPs) adopted in the fifth assessment report of the Intergovernmental Panel on Climate Change (IPCC). The RCPs are used to predict potential trends of atmospheric greenhouse gas concentrations based on different socio-economic factors.[85,86] These scenarios considered the effect of climate change and emission control regulations, and thus can be used to model the potential impacts of future anthropogenic emissions. In RCP 4.5, anthropogenic emissions of greenhouse gases are predicted to increase and peak in the 2030s ("stabilisation" scenario), while in RCP 8.5 emissions continually increase (i.e., a typical "business-as-usual" scenario).[87–91] We incorporated the ACCMIP modelling results into a global biogeochemical model

(COOLBEANS) to compute hypoxic areas under RCP 4.5 and 8.5 scenarios and the related change in N deposition. After discussing the limitations of the model, we analysed the impact of N-atmospheric on carbon fluxes and hypoxia as well as the temporal and spatial variability of the extent of hypoxia under ACCMIP results using RCP 4.5 and 8.5, which include both the effect of climate change and socio-economic factors on the deposition of N. Finally, we discuss the implication of our results with regard to the potential reduction of hypoxic areas following emission regulation and stabilisation of emission in China.

2. Materials and Methods

Estimating new marine primary productivity and associated carbon fluxes derived from total N deposition

We define "modern-day" N deposition based on the measurement of the atmospheric N deposition (dry and wet) described by Luo et al.[82]. They measured the N deposition in various coastal Chinese cities; Dalian, Changdao, Linshandao, Fenghua, Fuzhou and Zhanjiang (Figure 2). We assume a similar rate of N deposition in the coastal cities and the surrounding coastal Seas. We use the four coastal zones of China defined in COSCAT; East Yellow Sea, Bohai Sea, East China Sea and South China Sea as our study area (Table S1).[92,93] Thus, we take the average N deposition of the nearby coastal cities as "modern-day" N deposition in each study zones (Figure 2).

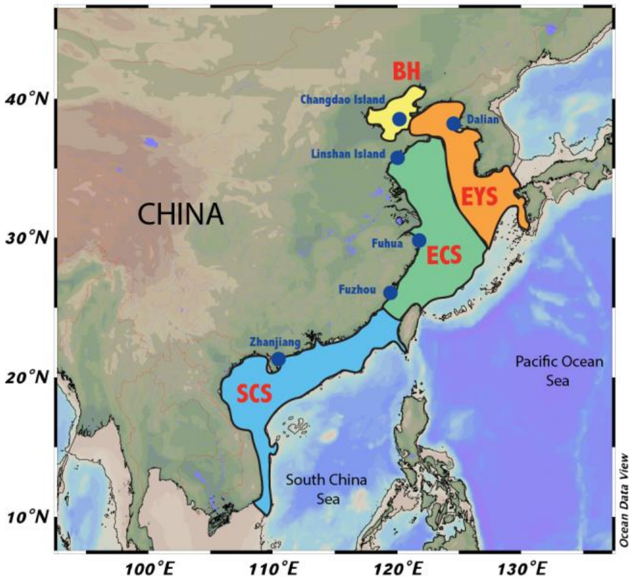

Figure 2. Coastal marine environments considered in this study. The East Yellow Sea (EYS), Bohai Sea (BH), East China Sea (ESC) and South China Sea (SCS) are defined in COSCAT (Table S1).[92] The circles represent coastal cities used in Luo et al.[82] to measure N deposition which is used in this study to establish the modern-day N deposition in each zones. This figure was created using Ocean Data View.[94]

To estimate future changes in N deposition in China, we used the projected percentage changes of dry and wet N deposition in the 2030s (2030-2039) and 2100s (2100-2109) under RCP4.5 and RCP8.5 scenarios reported in Zhang et al.[95], which used the results from ACCMIP models. The future scenarios considered both the impact of climate change and emissions. In the projection of future N deposition, the scenarios account for the change in both dry and wet deposition. Thus, changes in precipitation are included in our scenarios. Our study zones are slightly different from Zhang et al.[95] because we followed the COSCAT model[96] which accounts for river catchment and discharge. We therefore used the raw data provided by Zhang et al.[95] and recalculated the future percentage change of N deposition based on each COSCAT zones[96]. Then we averaged dry and wet N deposition and seasonal changes in each coastal ocean as the regional mean changes (in %) relative to the modern-day deposition (Table S3).

Using the modern-day N deposition measured by Luo et al.[82] and future average percentage change, we calculated the future N deposition (2030 and 2100) under RCP 4.5 and RCP 8.5 scenarios in each region. The difference of N deposition in each region between the future scenario (2030 and 2100) and modern-day scenario (2010) was then converted into changes in carbon flux using equation (1), assuming that all deposited N is assimilated by phytoplankton. It is further assumed that a C:N ratio in coastal and shelf systems is 10:1, which is slightly higher than 6.625 in the Redfield ratio because some of the nitrogen-rich organic matter is lost in the water column before sedimentary deposition.[93,97,98] Hence, carbon flux can be derived from the total N deposition according to

$$C = 10N$$

where C represents the carbon flux (mol C m^{-2} yr^{-1}) and N represents the N deposition (mol N m^{-2} yr^{-1}).

Calculating maximum hypoxic areas in the coastal Chinese seas

COOLBEANS (Coastal Ocean Oxygen Linked to Benthic Exchange And Nutrient Supply) is a model that links changes in nutrient fluxes with changes in coastal hypoxia.[93] The model quantifies bottom oxygen demand using relationships with aerobic respiration, organic matter decomposition, vertical exchange and iron and sulphate reduction. Parameters include water depth, surface salinity, surface temperature, primary productivity and surface oxygen for each zone to account for spatial variations (Table S2). Thus, it can be used to predict maximum coastal hypoxic areas under shifts in nutrient loads. COOLBEANS uses a modified version of the COSCAT zones and only consider the biochemically active part of the zone (i.e., the part where 80% of the productivity is located) to account for the fact that the impact on hypoxia will be concentrated where primary productivity is. A detailed description and validation of the model was published previously[93] and only the most important parts will be presented here, we refer the reader to the supplementary information and the original publication for more details. Here, we used COOLBEANS to estimate hypoxic areas caused by future changes in N deposition by applying changes in carbon fluxes calculated from modern-day and future N deposition (equations S1 to S5 in SI). We further compared the maximum hypoxic area from future scenarios and present-day hypoxic areas to assess the impacts of future N deposition on the area of hypoxia over coastal Chinese waters. Therefore, we assume riverine input remains constant in future scenarios in order to isolate the impact from atmospheric deposition. The uncertainty of the extent of hypoxic areas predicted for future scenarios is calculated based on the standard deviations of future N deposition in the ACCMIP models, which was reported in Zhang et al.[95].

Results

Calculation of new primary productivity and carbon fluxes derived from N deposition

In this study, we assumed that all N deposition in surface waters would be assimilated by phytoplankton and contributed to carbon fluxes.[93] We found that modern-day atmospheric N deposition would translate to a carbon flux of 25.6 g C m^{-2} yr^{-1} (East Yellow Sea), 28.1 g C m^{-2} yr^{-1} (Bohai Sea), 27.9 (East China Sea) and 37.0 g C m^{-2} yr^{-1} (South China Sea) (Figure 3), which indicates that the atmospheric deposition of N can support 2 to 12% of the total carbon flux. The East Yellow Sea has the highest percentage contribution of atmospheric to the total carbon flux (12.3%) (Table 1).

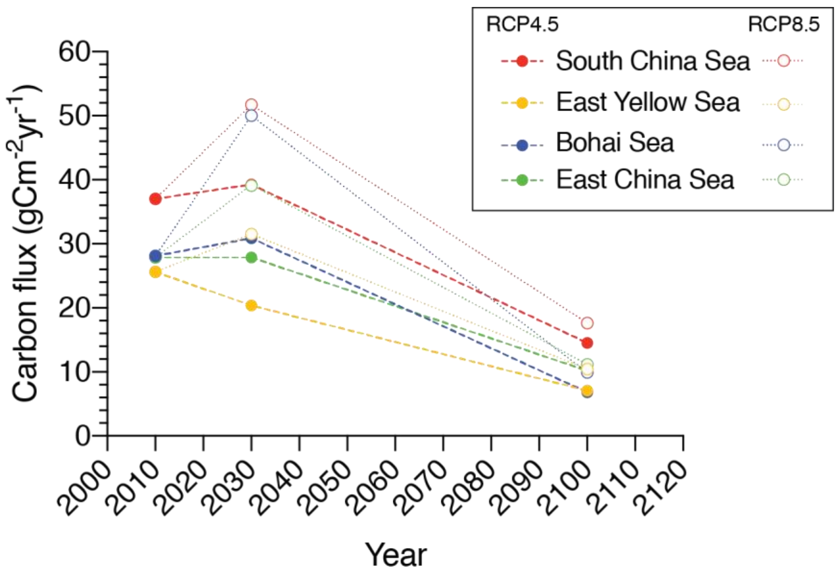

Figure 3. Modelled changes in carbon fluxes in Chinese coastal waters under RCP 4.5 (dots) and RCP 8.5 scenarios (open dots). All zones have higher carbon flux in 2030 under high atmospheric deposition (RCP 8.5) compared to 2010. We also note that in 2100 the carbon flux is lower is lower under both scenarios that includes emission regulation and climate change. Dots represent our modelled data and the dashed lines represent interpolation between our datapoint.

N deposition is shown to result in an increase in carbon fluxes in 2030 and a decrease in 2100 (Figure 3). We estimate the carbon flux to be 20.4 and 31.5 g C m^{-2} yr^{-1} (East Yellow Sea), 30.9 and 50.0 g C m^{-2} yr^{-1} (Bohai Sea), 27.5 and 39.2 g C m^{-2} yr^{-1} (East China Sea) and 51.7 and 59.3 g C m^{-2} yr^{-1} (South China Sea) in 2030 for scenarios RCP 4.5 and 8.5 respectively (Figure 3). All carbon fluxes are projected to peak in 2030, with the exception of the East China Sea, where the carbon flux decreased slightly (Figure 3). By 2100, the atmospheric contribution to the carbon flux decreased and was estimated to be 7.1 and 10.4 g C m^{-2} yr^{-1} (East Yellow Sea), 6.8 and 9.9 g C m^{-2} yr^{-1} (Bohai Sea), 10.2 and 11.2 g C m^{-2} yr^{-1} (East China Sea) and 17.6 and 14.5 g C m^{-2} yr^{-1} (South China Sea) for scenarios RCP 4.5 and 8.5 respectively. The Bohai Sea is the most affected area, with an increase in its carbon flux of 78% in 2030 and a decrease of 80% from 2030-2100 under RCP 8.5 (Figure 3). Overall, projected atmospheric N deposition would support between 2 – 15% and 1 – 6% of the total coastal carbon flux in 2030 and 2100 respectively.

Table 1. The contribution of atmospheric N deposition to the total carbon flux in each zone in percent

		RCP 4.5		RCP 8.5	
	Modern day	**2030**	**2100**	**2030**	**2100**
East Yellow Sea	12.3	9.8	3.4	15.2	5
Bohai Sea	2.1	2.3	0.5	3.7	0.7
East China Sea	4.4	4.4	1.6	5.2	1.8
South China Sea	8.5	11.9	6	13.3	4.8

Future changes in maximum hypoxic areas

Comparing to the modern-day maximum hypoxia area, projected maximum hypoxic areas in 2030 are estimated to change from -2.3% to +3.3% under RCP 4.5 and by +1.8% to +4.7% under RCP 8.5 depending on the region. Yet, by the end of 2100 the area affected by hypoxia is projected to decrease by 1.6% to 8.7% in RCP 4.5 and 1.3% to 7.1% in RCP 8.5 relative to the modern-day scenario due to a reduction in anthropogenic emissions reflecting predicted governmental regulations (Figure 4 and Table S3). Compared to the maximum hypoxic area reached in 2030, the hypoxia area of the China's coastal ocean decreases up to 6.6% under RCP 4.5 and up to 9.9% under RCP 8.5 by 2100. The South China Sea has the largest rate of change in hypoxia area per unit N loading (1.12 $km^2/mg\ N\ m^{-2}\ yr^{-1}$) followed by East Yellow Sea (0.96 $km^2/mg\ N\ m^{-2}\ yr^{-1}$), East China Sea (0.46 $km^2/mg\ N\ m^{-2}\ yr^{-1}$) and Bohai Sea (0.05 $km^2/mg\ N\ m^{-2}\ yr^{-1}$) (Table S3). Moreover, the South China Sea has the largest proportion of its biogeochemical active area that is hypoxia (31%) compared to other Chinese coastal oceans which is around 13%.

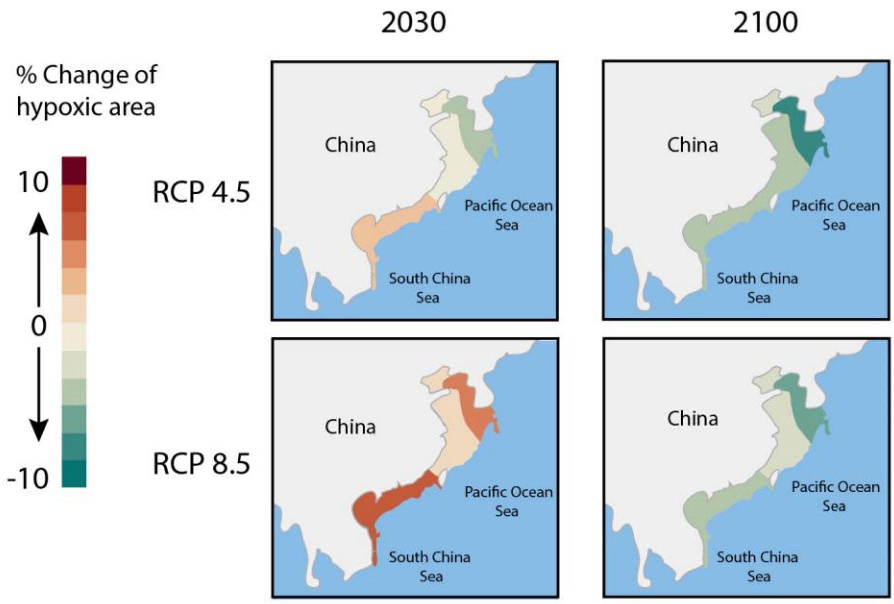

Figure 4. Modelled hypoxic areas (km^2) in Chinese coastal seas in modern-day and future N deposition under RCP 4.5 and RCP 8.5 emissions scenarios. The figure highlights the high sensitivity of dissolved oxygen to nitrogen load, especially in the South China Sea (left panels) but also the potential of improvement of water quality under emission reduction policy (right panels). This figure was created using Ocean Data View.[94]

Discussion

Impact of atmospheric deposition on primary productivity and carbon fluxes

Modern-day modelled atmospheric deposition accounts for about 30 g C m^{-2} yr^{-1} on average to the carbon flux in coastal Chinese waters (1.5 – 6.8 Tg C), which contributes to 2-12% of the total carbon flux (Figure 3). This is consistent with previous studies, whose estimations range from 2.3 to 68 g C m^{-2} yr^{-1}, contributing to 0.1 – 37% of the new primary productivity in the region.[54,56,99–101] This highlights the importance of atmospheric N deposition to the total carbon flux in coastal Chinese waters, and validates the effective performance of COOLBEANS in reproducing field data from this region.

Our calculations estimate that atmospheric input contributes around 12% of the total carbon flux in the East Yellow Sea, which is the highest among the coastal ocean in our study (Table

1). This may be explained by the low total carbon flux characteristic of the East Yellow Sea compared to other coastal zones, therefore the contribution of atmospheric input will be more significant in the region. Moreover, the East Yellow Sea is deeper than other sites considered here (150 m), which is used by COOLBEANS to calculate the total flux of organic carbon. Thus, the depth of the East Yellow Sea translates into a lower carbon flux compared to our other sites. These results highlight the spatial differences in the impact of changes in atmospheric deposition on the total carbon flux in Chinese coastal waters.

Temporal variation of coastal hypoxia

Under climatic scenarios RCP 4.5 and RCP 8.5, the average hypoxic areas in China coastal water will increase by about 1.6% relative to the modern-day by 2030. Our results are slightly higher but on the same order of magnitude as the modelled cumulative effect of climate change (increase air temperature of +3 °C) and river discharge (increase 10% of river discharge) reported by Lehrter et al.[102] in the Gulf of Mexico (+1%). This indicates that increases in atmospheric deposition due to human activity and climate change has an enhanced effect on the extent of hypoxia than climate change. For year 2100, we estimate an average decrease in carbon fluxes (-72% compared to modern-day) and thus hypoxia area (- 4%) in coastal Chinese waters under RCP 4.5 and RCP 8.5 scenarios. This decreasing trend is similar to Cabré et al.[103], who modelled a decrease of 37% in total primary productivity in the low-latitude upwelling area under climate change, which would also lead to a decrease in the area of hypoxia.

Our results suggest that hypoxic conditions will peak in 2030 and decrease in 2100, following the predicted trend of anthropogenic emissions. This illustrates how governmental control on emissions is important to control hypoxia. However, total N deposition and NO_X and NH_3 emissions in China began to stabilize in recent years, earlier than what RCP 4.5 and 8.5 predicted, due to stricter environmental policies in China.[104,105] While this doesn't change our quantification of the extent of hypoxia under a given reduction in N deposition, it could mean that the extent of hypoxic areas may start to stabilize and decrease earlier than 2030.

While scenarios RCP 4.5 and RCP 8.5 consider the effect of climate change on N deposition, physicochemical consequences of a warmer ocean are not included in COOLBEANS. Yet, impending sea surface warming may enhance stratification of water column and result in less mixing and oxygenation of bottom water, thereby increasing in the extent of coastal hypoxia.[27,103,106,107] Moreover, warmer ocean also decreases the solubility of oxygen and increase remineralization rate, which may further worsen the hypoxia.[107] Thus, our estimates might be considered conservative in this regard.

Spatial variation of sensitivity to nutrient input: The South China Sea

We observed spatial variation in forecasted future maximum hypoxic areas and their rates of change in coastal Chinese waters. The highest rate of hypoxia expansion per unit N added per year was found in the South China Sea, followed by the East Yellow Sea, East China Sea and Bohai Sea (Table S4). This can be attributed to the sensitivities of each respective coastal ocean to nutrient loading in COOLBEANS, which are mainly controlled by the bottom oxygen demand and vertical exchange of oxygen.[93] The bottom oxygen demand in the model is driven by depth and primary productivity in each zone. The South China Sea has a higher calculated bottom oxygen demand among the four zones in the model because of its relatively deep shelf and low vertical exchange of oxygen, resulting in lower modelled concentrations of bottom oxygen and a larger area of hypoxia.[13,45] Thus, controlling N input to the South China Sea, including atmospheric emissions, is critical to reduce coastal hypoxia. This is a grand challenge due to the densely populated regions on its coastline, including the Greater Bay Area, which houses about 120 million people and multiple industries. The high sensitivity of South China

Sea might increase when considered atmospheric inputs together with the effects of global warming such as enhanced stratification and the interplay of ongoing ocean acidification, eutrophication and hypoxia.[46]

Effect of a reduced emissions scenario on hypoxia

Hypoxia reduction targets should be set in China in order to reduce the ecological, social and economic impacts associated with the phenomenon. Taking the Gulf of Mexico as an example, the intergovernmental Gulf Task Force set a goal of reducing the hypoxic zone by about 70% (~5000 km^2 over a 5-year average) by 2035 in Gulf of Mexico and reducing 20% of the spring N loading from the Mississippi River.[108] Although this exact target may not be applicable in China, it can be used as a reference to evaluate measurable policy actions required to achieve acceptable reductions in N emissions and hypoxia. From our model, a reduction of 30 to 90% of N input, which includes atmospheric deposition and riverine inputs, is necessary to keep coastal hypoxic zones below 5000 km^2 in Chinese coastal waters. Therefore, strict controls on atmospheric emissions in China would have a substantial impact on the development of hypoxia in coastal waters.

Model limitations

While we took into consideration increase in N deposition due to both climate change (e.g., precipitation) and emission regulation, we do not include changes in riverine loads to predict its effects on future changes of hypoxic areas. Thus, our results might overlook the cumulative or competing effects of these parameters. Moreover, as highlighted before, COOLBEANS assumes that all nutrients will be assimilated and transferred to organic carbon. However, changes in nutrient loading may affect nutrient dynamics, plankton communities and the food web, which all play a role in coastal hypoxia formation.[27] While the efficiency of

COOLBEANS to reproduce observational data was previously demonstrated (Nash-Sutcliffee efficiency = 0.71), [93] the model does not consider seasonal and inter-annual physicochemical variability of the coastal environment but rather a yearly-averaged nitrogen deposition, primary productivity, carbon fluxes and biochemical oxygen demand. Thus, some discrepancy can be expected when comparing to field data that are often representing a snapshot in time. Our results should be considered as a first-order approximation for potential future trend in hypoxia under certain emissions scenarios, and therefore we focussed the discussion on relative change in the proportion of hypoxia over the biochemically active regions of COSCAT.

Atmospheric N deposition is a non-negligible source of nutrient supply from the land to coastal Chinese waters. Here, we quantified the impact of atmospheric N deposition on the extent of hypoxia in the coastal marine environment and highlighted regional differences in nutrient load sensitivities. This should serve as critical information when looking at N emissions control in nearby cities to avert the expansion of coastal hypoxia in China. Regions that are especially sensitive to N deposition, such as the South China Sea, should be prioritized. Implementing targets and emissions regulations in China is crucial to improve the water quality in coastal ecosystems.

Acknowledgement

Yau Yu Yan was partly funded by the Theme-based Research Scheme (T21-602/16-R) of the Hong Kong Research Grants Council co-awarded to DMB and the Stephen S.F. Hui Trust Fund awarded to BT. We thank Dr. Gao for providing the data of future changes in nitrogen deposition. We also thank John Doherty for proofreading. Data generated for this study are available in the supplementary material.

Supporting Information Available

Description of the COOLBEANS model; Input used to run the COOLBEANS model; Change of total deposition; Modelled change in hypoxic area; Modelled rate of change of hypoxia

References

(1) Galloway, J. N.; Winiwarter, W.; Leip, A.; Leach, A. M.; Bleeker, A.; Erisman, J. W. Nitrogen Footprints: Past, Present and Future. *Environ. Res. Lett.* **2014**, *9* (11), 115003. https://doi.org/10.1088/1748-9326/9/11/115003.

(2) Kanakidou, M.; Myriokefalitakis, S.; Daskalakis, N.; Fanourgakis, G.; Nenes, A.; Baker, A. R.; Tsigaridis, K.; Mihalopoulos, N. Past, Present, and Future Atmospheric Nitrogen Deposition. *J. Atmos. Sci.* **2016**, *73* (5), 2039–2047. https://doi.org/10.1175/JAS-D-15-0278.1.

(3) Dentener, F.; Drevet, J.; Lamarque, J. F.; Bey, I.; Eickhout, B.; Fiore, A. M.; Hauglustaine, D.; Horowitz, L. W.; Krol, M.; Kulshrestha, U. C.; Lawrence, M Galy-Lacaux, C.; Rast, S.; Shindell, D.; Stevenson, D.; Van Noije, T.; Atherton, C. Bell, N.; Bergman, D.; Butler, T.; Cofala, J.; Collins, B.; Doherty, R.; Ellingsen, K.; Galloway, J.; Gauss, Michael.; Montanaro, V.; Müller, J. F.; Pitari, G.; Rodriguez, J. Sanderson, M.; Solmon, F.; Strahan, S.; Schultz, M.; Sudo, K.; Szopa, S.; Wild, O. Nitrogen and Sulfur Deposition on Regional and Global Scales: A Multimodel Evaluation. *Global Biogeochem. Cycles* **2006**, *20* (4), GB4003. https://doi.org/10.1029/2005GB002672.

(4) Graneli, E.; Wallstrom, K.; Larsson, U.; Graneli, W.; Elmgren, R. Nutrient Limitation of Primary Production in the Baltic Sea Area. *Ambio* **1990**, *19* (3), 142–151.

(5) Howarth, R. W.; Marino, R. Nitrogen as the Limiting Nutrient for Eutrophication in Coastal Marine Ecosystems: Evolving Views over Three Decades. *Limnol. Oceanogr.* **2006**, *51* (1part2), 364–376. https://doi.org/10.4319/lo.2006.51.1_part_2.0364.

(6) Voss, M.; Bange, H. W.; Dippner, J. W.; Middelburg, J. J.; Montoya, J. P.; Ward, B. The Marine Nitrogen Cycle : Recent Discoveries , Uncertainties and the Potential Relevance of Climate Change The Marine Nitrogen Cycle : Recent Discoveries , Uncertainties and the Potential Relevance of Climate Change. *Phil Trans R Soc B* **2013**, *368* (1621).

(7) Paerl, H. W. Coastal Eutrophication and Harmful Algal Blooms: Importance of Atmospheric Deposition and Groundwater as “new” Nitrogen and Other Nutrient Sources. *Limnol. Oceanogr.* **1997**, *42* (5), 1154–1165.

(8) Galloway, J. N.; Dentener, F. J.; Capone, D. G.; Boyer, E. W.; Howarth, R. W.; Seitzinger, S. P.; Asner, G. P.; Cleveland, C. C.; Green, P. A.; Holland, E. A.; Karl, D. M.; Michaels, A. F.; Porter, J. H.; Townsend, A. R.; Vörösmarty, C. J. Nitrogen Cycles: Past, Present, and Future. *Biogeochemistry* **2004**, *70* (2), 153–226. https://doi.org/10.1007/s10533-004-0370-0.

(9) Troost, T. A.; Blaas, M.; Los, F. J. The Role of Atmospheric Deposition in the Eutrophication of the North Sea: A Model Analysis. *J. Mar. Syst.* **2013**, *125*, 101–112. https://doi.org/10.1016/j.jmarsys.2012.10.005.

(10) Thibodeau, B.; Helie, J.; Lehmann, M. F. Variations of the Nitrate Isotopic

Composition in the St . Lawrence River Caused by Seasonal Changes in Atmospheric Nitrogen Inputs. *Biogeochemistry* **2013**, *115*, 287–298. https://doi.org/10.1007/s10533-013-9834-4.

(11) Gao, Y.; Zhou, F.; Ciais, P.; Miao, C.; Yang, T.; Jia, Y.; Zhou, X.; Klaus, B.-B.; Yu, G.; Yang, T. Human Activities Aggravate Nitrogen Deposition Pollution to Inland Water over China. *Natl. Sci. Rev.* **2019**, No. June, 1–11. https://doi.org/10.1093/nsr/nwz073.

(12) Zhang, Y.; Liu, C.; Liu, X.; Xu, W.; Wen, Z. Atmospheric Nitrogen Deposition around the Dongting Lake, China. *Atmos. Environ.* **2019**, *207* (March), 197–204. https://doi.org/10.1016/j.atmosenv.2019.03.034.

(13) Dai, M.; Cai, P.; Zhai, W.; Tang, T.; Wang, L.; Cai, W.-J.; Wang, B.; Yuan, L.; Guo, X. Oxygen Depletion in the Upper Reach of the Pearl River Estuary during a Winter Drought. *Mar. Chem.* **2006**, *102* (1–2), 159–169. https://doi.org/10.1016/j.marchem.2005.09.020.

(14) Da, F.; Friedrichs, M. A. M.; St-Laurent, P. Impacts of Atmospheric Nitrogen Deposition and Coastal Nitrogen Fluxes on Oxygen Concentrations in Chesapeake Bay. *J. Geophys. Res. Ocean.* **2018**, *123* (7), 5004–5025. https://doi.org/10.1029/2018JC014009.

(15) Zhang, H.; Li, S. Effects of Physical and Biochemical Processes on the Dissolved Oxygen Budget for the Pearl River Estuary during Summer. *J. Mar. Syst.* **2010**, *79* (1–2), 65–88. https://doi.org/10.1016/j.jmarsys.2009.07.002.

(16) Duce, R. A.; LaRoche, J.; Altieri, K.; Arrigo, K. R.; Baker, A. R.; Capone, D. G.; Cornell, S.; Dentener, F.; Galloway, J.; Ganeshram, R. S.; Geider, R. J.; Jickells, T.Kuypers, M. M.; Langlois, R.; Liss, P. S.; Liu, S. M.; Middelburg, J. J.; Moore, C. M.; Nickovic, S.; Oschlies, A.; Pedersen, T.; Prospero, J.; Schlitzer, R.; Seitzinger, S.; Sorensen, L. L.; Uematsu, M.; Ulloa, O.; Voss, M.; Ward, B.; Zamora, L. Impacts of Atmospheric Anthropogenic Nitrogen on the Open Ocean. *Science (80-.).* **2008**, *320* (5878), 893–897. https://doi.org/10.1126/science.1150369.

(17) St-Laurent, P.; Friedrichs, M. A. M.; Najjar, R. G.; Martins, D. K.; Herrmann, M.; Miller, S. K.; Wilkin, J. Impacts of Atmospheric Nitrogen Deposition on Surface Waters of the Western North Atlantic Mitigated by Multiple Feedbacks. *J. Geophys. Res. Ocean.* **2017**, *122* (11), 8406–8426. https://doi.org/10.1002/2017JC013072.

(18) Jickells, T. D.; Buitenhuis, E.; Altieri, K.; Baker, A. R.; Capone, D.; Duce, R. A.; Dentener, F.; Fennel, K.; Kanakidou, M.; LaRoche, J.; Lee, K; Liss, P.; Middelburg, J. J.; Moore, J. K.; Okin, G.; Oschlies, A.; Sarin, M.; Seitzinger, S.; Sharples, J.; Singh, A.; Suntharalingam, P.; Uematsu, M.; Zamora, L. M. A Reevaluation of the Magnitude and Impacts of Anthropogenic Atmospheric Nitrogen Inputs on the Ocean. *Global Biogeochem. Cycles* **2017**, *31* (2), 289–305. https://doi.org/10.1002/2016GB005586.

(19) Liu, L.; Zhang, X.; Wang, S.; Lu, X.; Ouyang, X. A Review of Spatial Variation of Inorganic Nitrogen (N) Wet Deposition in China. *PLoS ONE*. 2016, pp 1–17. https://doi.org/10.1371/journal.pone.0146051.

(20) Kim, T. W.; Lee, K.; Duce, R.; Liss, P. Impact of Atmospheric Nitrogen Deposition on Phytoplankton Productivity in the South China Sea. *Geophys. Res. Lett.* **2014**, *41* (9), 3156–3162. https://doi.org/10.1002/2014GL059665.

(21) Nixon, S. W. Coastal Marine Eutrophication: A Definition, Social Causes, and Future Concerns. *Ophelia* **1995**, *41* (1), 199–219. https://doi.org/10.1080/00785236.1995.10422044.

(22) Nixon, S. W. Eutrophication and the Macroscope. *Hydrobiologia* **2009**, *629* (1), 5–19. https://doi.org/10.1007/s10750-009-9759-z.

(23) Erisman, J. W.; Galloway, J.; Seitzinger, S.; Bleeker, A.; Butterbach-Bahl, K. Reactive

Nitrogen in the Environment and Its Effect on Climate Change. *Curr. Opin. Environ. Sustain.* **2011**, *3* (5), 281–290. https://doi.org/10.1016/j.cosust.2011.08.012.

(24) Cole, J. J.; Findlay, S.; Pace, M. L. Bacterial Production in Fresh and Saltwater Ecosystem: A Cross-System Overview. *Mar. Ecol. - Prog. Ser.* **1988**, *43*, 1–10.

(25) Diaz, R. J.; Rosenberg, R. Marine Benthic Hypoxia : A Review of Its Ecological Effects and the Behavioural Responses of Benthic Macrofauna. *Oceanogr. Mar. Biol. an Annu. Rev.* **1995**, *33*, 245–303. https://doi.org/10.1021/je700185m.

(26) Fennel, K.; Levin, J.; Moisan, J.; Wilkin, J.; O'Reilly, J.; Haidvogel, D. Nitrogen Cycling in the Middle Atlantic Bight: Results from a Three-Dimensional Model and Implications for the North Atlantic Nitrogen Budget. *Global Biogeochem. Cycles* **2006**, *20* (3), GB3007. https://doi.org/10.1029/2005gb002456.

(27) Diaz, R. J.; Rosenberg, R. Spreading Dead Zones and Consequences for Marine Ecosystems. *Science (80-.).* **2008**, *321* (5891), 926–929. https://doi.org/10.1126/science.1156401.

(28) Thibodeau, B.; de Vernal, A.; Mucci, A. Recent Eutrophication and Consequent Hypoxia in the Bottom Waters of the Lower St. Lawrence Estuary: Micropaleontological and Geochemical Evidence. *Mar. Geol.* **2006**, *231* (1–4), 37–50. https://doi.org/10.1016/j.margeo.2006.05.010.

(29) Collos, Y.; Döhler, G.; Biermann, I. Production of Dissolved Organic Nitrogen during Uptake of Nitrate by Synedra Planctonica: Implications for Estimates of New Production in the Oceans. *J. Plankton Res.* **1992**, *14* (8), 1025–1029. https://doi.org/10.1093/plankt/14.8.1025.

(30) Seitzinger, S. P.; Harrison, J. A.; Böhlke, J. K.; Bouwman, A. F.; Lowrance, R.; Tobias, C.; Drecht, G. Van. Denitrification across Landscapes and Waterscapes : A Synthesis. *Ecol. Appl.* **2006**, *16* (6), 2064–2090.

(31) Galloway, J. N.; Erisman, J. W.; Howarth, R. W.; Cowling, E. B.; Aber, J. D.; Cosby, B. J.; Seitzinger, S. P. The Nitrogen Cascade. *Bioscience* **2003**, *53* (4), 341–356. https://doi.org/10.1641/0006-3568(2003)053[0341:tnc]2.0.co;2.

(32) Diaz, R. J. Overview of Hypoxia around the World. *J. Environ. Qual.* **2001**, *30* (2), 275–281.

(33) Pena, M. A.; Katsev, S.; Oguz, T.; Gilbert, D. Modeling Dissolved Oxygen Dynamics and Hypoxia. *Biogeosciences* **2010**, *7*, 933–957.

(34) Conley, D. J.; Destouni, G.; Gustafsson, B. O. G.; Hietanen, S.; Kortekaas, M.; Kuosa, H.; Meier, H. E. M.; Norkko, A. L. F.; Gertrud, N. U.; Rosenberg, R.; Savchuk, O. P.; Slomp, C. P.; Voss, M. Hypoxia-Related Processes in the Baltic Sea. *Environ. Sci. Technol.* **2009**, *43* (10), 3412–3420.

(35) Dodds, W. K. Nutrients and the "Dead Zone": The Link between Nutrient Ratios and Dissolved Oxygen in the Northern Gulf of Mexico. *Ecol. Soc. Am.* **2006**, *14* (1), 3–4.

(36) Murphy, R. R.; Kemp, W. M.; Ball, W. P. Long-Term Trends in Chesapeake Bay Seasonal Hypoxia, Stratification, and Nutrient Loading. *Estuaries and Coasts* **2011**, *34* (6), 1293–1309. https://doi.org/10.1007/s12237-011-9413-7.

(37) Gilbert, D.; Sundby, B.; Gobeil, C.; Mucci, A.; Tremblay, G.-H. A Seventy-Two-Year Record of Diminishing Deep-Water Oxygen in the St. Lawrence Estuary: The Northwest Atlantic Connection. *Am. Soc. Linmnology Oceanogr.* **2005**, *50* (5), 1654–1666.

(38) Huang, L.; Smith, M. D.; Craig, J. K. Quantifying the Economic Effects of Hypoxia on a Fishery for Brown Shrimp Farfantepenaeus Aztecus. *Mar. Coast. Fish.* **2010**, *2* (1), 232–248. https://doi.org/10.1577/c09-048.1.

(39) Rabotyagov, S. S.; Kling, C. L.; Gassman, P. W.; Rabalais, N. N.; Turner, R. E. The Economics of Dead Zones: Causes, Impacts, Policy Challenges, and a Model of the

Gulf of Mexico Hypoxic Zone. *Rev. Environ. Econ. Policy* **2014**, *8* (1), 58–79. https://doi.org/10.1093/reep/ret024.
(40) Breitburg, D.; Levin, L. A.; Oschlies, A.; Grégoire, M.; Chavez, F. P.; Conley, D. J.; Garçon, V.; Gilbert, D.; Gutiérrez, D.; Isensee, K.; Jacinto, G. S.; Limburg, K. E.; Montes, I.; Naqvi, S. W.A.; Pitcher, G. C.; Rabalais, N. N.; Roman, M. R.; Rose, K. A.; Seibel, B. A.; Telszewski, M.; Yasuhara, M.; Zhang, J. Declining Oxygen in the Global Ocean and Coastal Waters. *Science (80-.).* **2018**, *359* (6371), 46. https://doi.org/10.1126/science.aam7240.
(41) Zhang, J.; Gilbert, D.; Gooday, A. J.; Levin, L.; Naqvi, S. W. A.; Middelburg, J. J.; Scranton, M.; Ekau, W.; Peña, A.; Dewitte, B.; Oguz, T.; Monteiro, P. M.S.; Urban, E.; Rabalais, N. N.; Ittekkot, V.; Kemp, W. M.; Ulloa, O.; Elmgren, R.; Escobar-Briones, E.; Van Der Plas, A. K. Natural and Human-Induced Hypoxia and Consequences for Coastal Areas: Synthesis and Future Development. *Biogeosciences* **2010**, *7* (5), 1443–1467. https://doi.org/10.5194/bg-7-1443-2010.
(42) Phoenix, G. K.; Emmett, B. A.; Britton, A. J.; Caporn, S. J. M.; Dise, N. B.; Helliwell, R.; Jones, L.; Leake, J. R.; Leith, I. D.; Sheppard, L. J.; Sowerby, A.; Pilkington, M. G.; Rowe, E. C.; Ashmore, M. R.; Power, S. A. Impacts of Atmospheric Nitrogen Deposition: Responses of Multiple Plant and Soil Parameters across Contrasting Ecosystems in Long-Term Field Experiments. *Glob. Chang. Biol.* **2012**, *18* (4), 1197–1215. https://doi.org/10.1111/j.1365-2486.2011.02590.x.
(43) Howarth, R. W.; Sharpley, A.; Walker, D. Sources of Nutrient Pollution to Coastal Waters in the United States : Implications for Achieving Coastal Water Quality Goals. *Estuaries* **2002**, *25* (4), 656–676.
(44) Zhang, J.; Liu, S. M.; Ren, J. L.; Wu, Y.; Zhang, G. L. Nutrient Gradients from the Eutrophic Changjiang (Yangtze River) Estuary to the Oligotrophic Kuroshio Waters and Re-Evaluation of Budgets for the East China Sea Shelf. *Prog. Oceanogr.* **2007**, *74* (4), 449–478. https://doi.org/10.1016/j.pocean.2007.04.019.
(45) Lu, Z.; Gan, J.; Dai, M.; Liu, H.; Zhao, X. Joint Effects of Extrinsic Biophysical Fluxes and Intrinsic Hydrodynamics on the Formation of Hypoxia West off the Pearl River Estuary. *J. Geophys. Res. Ocean.* **2018**, *123* (9), 6241–6259. https://doi.org/10.1029/2018JC014199.
(46) Qian, W.; Gan, J.; Liu, J.; He, B.; Lu, Z.; Guo, X.; Wang, D.; Guo, L.; Huang, T.; Dai, M. Current Status of Emerging Hypoxia in a Eutrophic Estuary: The Lower Reach of the Pearl River Estuary, China. *Estuar. Coast. Shelf Sci.* **2018**, *205*, 58–67. https://doi.org/10.1016/j.ecss.2018.03.004.
(47) Tang, D.; Di, B.; Wei, G.; Ni, I.; Oh, I. S.; Wang, S. Spatial , Seasonal and Species Variations of Harmful Algal Blooms in the South Yellow Sea and East China Sea. *Hydrobiologia* **2006**, *568*, 245–253. https://doi.org/10.1007/s10750-006-0108-1.
(48) Hu, C.; Li, D.; Chen, C.; Ge, J.; Muller-Karger, F. E.; Liu, J.; Yu, F.; He, M. X. On the Recurrent Ulva Prolifera Blooms in the Yellow Sea and East China Sea. *J. Geophys. Res. Ocean.* **2010**, *115* (5). https://doi.org/10.1029/2009JC005561.
(49) Zhu, Z. Y.; Wu, H.; Liu, S. M.; Wu, Y.; Huang, D. J.; Zhang, J.; Zhang, G. Sen. Hypoxia off the Changjiang (Yangtze River) Estuary and in the Adjacent East China Sea: Quantitative Approaches to Estimating the Tidal Impact and Nutrient Regeneration. *Mar. Pollut. Bull.* **2017**, *125* (1–2), 103–114. https://doi.org/10.1016/j.marpolbul.2017.07.029.
(50) Chen, C. C.; Gong, G. C.; Shiah, F. K. Hypoxia in the East China Sea: One of the Largest Coastal Low-Oxygen Areas in the World. *Mar. Environ. Res.* **2007**, *64* (4), 399–408. https://doi.org/10.1016/j.marenvres.2007.01.007.
(51) Zhu, Y.; Mccowan, A.; Cook, P. L. M. Effects of Changes in Nutrient Loading and

Composition on Hypoxia Dynamics and Internal Nutrient Cycling of a Stratified Coastal Lagoon. *Biogeosciences* **2017**, *14*, 4423–4433.

(52) Archana, A.; Thibodeau, B.; Geeraert, N.; Xu, M. N.; Kao, S. J.; Baker, D. M. Nitrogen Sources and Cycling Revealed by Dual Isotopes of Nitrate in a Complex Urbanized Environment. *Water Res.* **2018**, *142*, 459–470. https://doi.org/10.1016/j.watres.2018.06.004.

(53) Archana, A.; Li, L.; Shuh-Ji, K.; Thibodeau, B.; Baker, D. M. Variations in Nitrate Isotope Composition of Wastewater Effluents by Treatment Type in Hong Kong. *Mar. Pollut. Bull.* **2016**, *111* (1–2), 143–152. https://doi.org/10.1016/j.marpolbul.2016.07.019.

(54) Zhang, Y.; Yu, Q.; Ma, W.; Chen, L. Atmospheric Deposition of Inorganic Nitrogen to the Eastern China Seas and Its Implications to Marine Biogeochemistry. *J. Geophys. Res. Atmos.* **2010**, *115* (11), 1–10. https://doi.org/10.1029/2009JD012814.

(55) Yang, J. Y. T.; Hsu, S. C.; Dai, M. H.; Hsiao, S. S. Y.; Kao, S. J. Isotopic Composition of Water-Soluble Nitrate in Bulk Atmospheric Deposition at Dongsha Island: Sources and Implications of External N Supply to the Northern South China Sea. *Biogeosciences* **2014**, *11* (7), 1833–1846. https://doi.org/10.5194/bg-11-1833-2014.

(56) De Leeuw, G.; Spokes, L.; Jickells, T.; Skjøth, C. A.; Hertel, O.; Vignati, E.; Tamm, S.; Schulz, M.; Sørensen, L. L.; Pedersen, B.; Klein, L.; Heinke Schlünzen, K. Atmospheric Nitrogen Inputs into the North Sea: Effect on Productivity. *Cont. Shelf Res.* **2003**, *23* (17–19), 1743–1755. https://doi.org/10.1016/j.csr.2003.06.011.

(57) Wang, M.; Ma, L.; Strokal, M.; Ma, W.; Liu, X.; Kroeze, C. Hotspots for Nitrogen and Phosphorus Losses from Food Production in China: A County-Scale Analysis. *Environ. Sci. Technol.* **2018**, *52* (10), 5782–5791. https://doi.org/10.1021/acs.est.7b06138.

(58) Liu, X.; Duan, L.; Mo, J.; Du, E.; Shen, J.; Lu, X.; Zhang, Y.; Zhou, X.; He, C.; Zhang, F. Nitrogen Deposition and Its Ecological Impact in China: An Overview. *Environ. Pollut.* **2011**, *159* (10), 2251–2264. https://doi.org/10.1016/j.envpol.2010.08.002.

(59) Zhao, B.; Wang, S. X.; Liu, H.; Xu, J. Y.; Fu, K.; Klimont, Z.; Hao, J. M.; He, K. B.; Cofala, J.; Amann, M. NOx Emissions in China: Historical Trends and Future Perspectives. *Atmos. Chem. Phys.* **2013**, *13* (19), 9869–9897. https://doi.org/10.5194/acp-13-9869-2013.

(60) Xie, Y.; Xiong, Z.; Xing, G.; Yan, X.; Shi, S.; Sun, G.; Zhu, Z. Source of Nitrogen in Wet Deposition to a Rice Agroecosystem at Tai Lake Region. *Atmos. Environ.* **2008**, *42* (21), 5182–5192. https://doi.org/10.1016/j.atmosenv.2008.03.008.

(61) Xu, W.; Zhao, Y.; Liu, X.; Dore, A. J.; Zhang, L.; Liu, L.; Cheng, M. Atmospheric Nitrogen Deposition in the Yangtze River Basin: Spatial Pattern and Source Attribution. *Environ. Pollut.* **2018**, *232*, 546–555. https://doi.org/10.1016/j.envpol.2017.09.086.

(62) Zhang, J.; Zhang, G. S.; Bi, Y. F.; Liu, S. M. Nitrogen Species in Rainwater and Aerosols of the Yellow and East China Seas: Effects of the East Asian Monsoon and Anthropogenic Emissions and Relevance for the NW Pacific Ocean. *Global Biogeochem. Cycles* **2011**, *25* (3), 1–15. https://doi.org/10.1029/2010GB003896.

(63) Wang, X.; Wu, Z.; Shao, M.; Fang, Y.; Zhang, L.; Chen, F.; Chan, P.; Fan, Q.; Wang, Q.; Zhu, S.; Bao, R. Atmospheric Nitrogen Deposition to Forest and Estuary Environments in the Pearl River Delta Region, Southern China. *Tellus B* **2013**, *65*, 1–13. https://doi.org/10.3402/tellusb.v65i0.20480.

(64) Uno, I.; Uematsu, M.; Hara, Y.; He, Y. J.; Ohara, T.; Mori, A.; Kamaya, T.; Murano, K.; Sadanaga, Y.; Bandow, H. Numerical Study of the Atmospheric Input of

Anthropogenic Total Nitrate to the Marginal Seas in the Western North Pacific Region. *Geophys. Res. Lett.* **2007**, *34* (17). https://doi.org/10.1029/2007GL030338.

(65) Zhao, Y.; Zhang, L.; Pan, Y.; Wang, Y.; Paulot, F.; Henze, D. K. Atmospheric Nitrogen Deposition to the Northwestern Pacific: Seasonal Variation and Source Attribution. *Atmos. Chem. Phys.* **2015**, *15* (18), 10905–10924. https://doi.org/10.5194/acp-15-10905-2015.

(66) Kim, T. W.; Lee, K.; Najjar, R. G.; Jeong, H. D.; Jeong, H. J. Increasing N Abundance in the Northwestern Pacific Ocean due to Atmospheric Nitrogen Deposition. *Science (80-.).* **2011**, *334* (6055), 505–509. https://doi.org/10.1126/science.1206583.

(67) Cui, S.; Shi, Y.; Groffman, P. M.; Schlesinger, W. H.; Zhu, Y. Centennial-Scale Analysis of the Creation and Fate of Reactive Nitrogen in China (1910-2010). *Proc. Natl. Acad. Sci. U. S. A.* **2013**, *110* (6), 2052–2057. https://doi.org/10.1073/pnas.1221638110.

(68) Liu, X.; Zhang, Y.; Han, W.; Tang, A.; Shen, J.; Cui, Z.; Vitousek, P.; Erisman, J. W.; Goulding, K.; Christie, P.; Fangmeier, A.; Zhang, F. Enhanced Nitrogen Deposition over China. *Nature* **2013**, *494* (7438), 459–462. https://doi.org/10.1038/nature11917.

(69) Kim, T. H.; Kim, G. Changes in Seawater N: P Ratios in the Northwestern Pacific Ocean in Response to Increasing Atmospheric N Deposition: Results from the East (Japan) Sea. *Limnol. Oceanogr.* **2013**, *58* (6), 1907–1914. https://doi.org/10.4319/lo.2013.58.6.1907.

(70) Grosse, J.; Bombar, D.; Doan, H. N.; Nguyen, L. N.; Voss, M. The Mekong River Plume Fuels Nitrogen Fixation and Determines Phytoplankton Species Distribution in the South China Sea during Low- and High-Discharge Season. *Limnol. Oceanogr.* **2010**, *55* (4), 1668–1680. https://doi.org/10.4319/lo.2010.55.4.1668.

(71) Yin, K.; Qian, P. Y.; Wu, M. C. S.; Chen, J. C.; Huang, L.; Song, X.; Jian, W. Shift from P to N Limitation of Phytoplankton Growth across the Pearl River Estuarine Plume during Summer. *Mar. Ecol. Prog. Ser.* **2001**, *221*, 17–28. https://doi.org/10.3354/meps221017.

(72) Hu, J.; Peng, P.; Jia, G.; Mai, B.; Zhang, G. Distribution and Sources of Organic Carbon, Nitrogen and Their Isotopes in Sediments of the Subtropical Pearl River Estuary and Adjacent Shelf, Southern China. *Mar. Chem.* **2006**, *98* (2–4), 274–285. https://doi.org/10.1016/j.marchem.2005.03.008.

(73) Wang, B. D.; Wang, X. L.; Zhan, R. Nutrient Conditions in the Yellow Sea and the East China Sea. *Estuar. Coast. Shelf Sci.* **2003**, *58* (1), 127–136. https://doi.org/10.1016/S0272-7714(03)00067-2.

(74) Kanakidou, M.; Tsigaridis, K.; Mahowald, N.; Baker, A. R.; Hunter, K. A.; Sarin, M.; Duce, R. A.; Zhu, T.; Liss, P. S.; Zamora, L. M.; Dentener, F. J.; Benitez-Nelson, C.; Okin, G. S.; Uematsu, M.; Prospero, J. M. Atmospheric Fluxes of Organic N and P to the Global Ocean. *Global Biogeochem. Cycles* **2012**, *26* (3), 1–12. https://doi.org/10.1029/2011gb004277.

(75) Nydahl, A.; Panigrahi, S.; Wikner, J. Increased Microbial Activity in a Warmer and Wetter Climate Enhances the Risk of Coastal Hypoxia. *FEMS Microbiol. Ecol.* **2013**, *85* (2), 338–347. https://doi.org/10.1111/1574-6941.12123.

(76) Veraart, A. J.; de Klein, J. J. M.; Scheffer, M. Warming Can Boost Denitrification Disproportionately due to Altered Oxygen Dynamics. *PLoS One* **2011**, *6* (3), 2–7. https://doi.org/10.1371/journal.pone.0018508.

(77) Kryza, M.; Werner, M.; Dore, A. J.; BłaŚ, M.; Sobik, M. The Role of Annual Circulation and Precipitation on National Scale Deposition of Atmospheric Sulphur and Nitrogen Compounds. *J. Environ. Manage.* **2012**, *109* (x), 70–79. https://doi.org/10.1016/j.jenvman.2012.04.048.

(78) Wałaszek, K.; Kryza, M.; Dore, A. J. The Impact of Precipitation on Wet Deposition of Sulphur and Nitrogen Compounds. *Ecol. Chem. Eng. S* **2013**, *20* (4), 733–745. https://doi.org/10.2478/eces-2013-0051.
(79) Chong-Hai, X.; Ying, X. The Projection of Temperature and Precipitation over China under RCP Scenarios Using a CMIP5 Multi-Model Ensemble. *Atmos. Ocean. Sci. Lett.* **2012**, *5* (6), 527–533. https://doi.org/10.1080/16742834.2012.11447042.
(80) Wang, L.; Chen, W. A CMIP5 Multimodel Projection of Future Temperature, Precipitation, and Climatological Drought in China. *Int. J. Climatol.* **2014**, *34* (6), 2059–2078. https://doi.org/10.1002/joc.3822.
(81) Sinha, E.; Michalak, A. M.; Balaji, V. Eutrophication Will Increase during the 21st Century as a Result of Precipitation Changes. *Science (80-.).* **2017**, *357* (6349), 405–408. https://doi.org/10.1126/science.aan2409.
(82) Luo, X. S.; Tang, A. H.; Shi, K.; Wu, L. H.; Li, W. Q.; Shi, W. Q.; Shi, X. K.; Erisman, J. W.; Zhang, F. S.; Liu, X. J. Chinese Coastal Seas Are Facing Heavy Atmospheric Nitrogen Deposition. *Environ. Res. Lett.* **2014**, *9* (9). https://doi.org/10.1088/1748-9326/9/9/095007.
(83) Chen, N.; Hong, H.; Huang, Q.; Wu, J. Atmospheric Nitrogen Deposition and Its Long-Term Dynamics in a Southeast China Coastal Area. *J. Environ. Manage.* **2011**, *92* (6), 1663–1667. https://doi.org/10.1016/j.jenvman.2011.01.026.
(84) Taketani, F.; Aita, M. N.; Yamaji, K.; Sekiya, T.; Ikeda, K.; Sasaoka, K.; Hashioka, T.; Honda, M. C.; Matsumoto, K.; Kanaya, Y. Seasonal Response of North Western Pacific Marine Ecosystems to Deposition of Atmospheric Inorganic Nitrogen Compounds from East Asia. *Sci. Rep.* **2018**, *8* (1), 1–9. https://doi.org/10.1038/s41598-018-27523-w.
(85) van Vuuren, D. P.; Edmonds, J.; Kainuma, M.; Riahi, K.; Thomson, A.; Hibbard, K.; Hurtt, G. C.; Kram, T.; Krey, V.; Lamarque, J. F.; Masui, T.; Meinshausen, M.; Nakicenovic, N.; Smith, S. J.; Rose, S. K. The Representative Concentration Pathways: An Overview. *Clim. Change* **2011**, *109* (1), 5–31. https://doi.org/10.1007/s10584-011-0148-z.
(86) IPCC. *Climate Change 2014: Synthesis Report*; IPCC: Geneva, Switzerland, 2014. https://doi.org/10.1046/j.1365-2559.2002.1340a.x.
(87) Clarke, L.; Edmonds, J.; Jacoby, H.; Pitcher, H.; Reilly, J.; Richels, R. *Scenarios of Greenhouse Gas Emissions and Atmospheric Concentrations. Sub-Report 2.1A of Synthesis and Assessment Product 2.1 by the U.S. Climate Change Science Program and the Subcommittee on Global Change Research*; 2007.
(88) Wise, M.; Calvin, K.; Thomson, A.; Clarke, L.; Bond-lamberty, B.; Sands, R.; Smith, S. J.; Janetos, A.; Edmonds, J. Implications of Limiting CO2 Concentrations for Land Use and Energy. *Science (80-.).* **2009**, *1183* (2), 1183–1187. https://doi.org/10.1126/science.1168475.
(89) Riahi, K.; Grübler, A.; Nakicenovic, N. Scenarios of Long-Term Socio-Economic and Environmental Development under Climate Stabilization. *Technol. Forecast. Soc. Change* **2007**, *74* (7), 887–935. https://doi.org/10.1016/j.techfore.2006.05.026.
(90) Thomson, A. M.; Calvin, K. V.; Smith, S. J.; Kyle, G. P.; Volke, A.; Patel, P.; Delgado-Arias, S.; Bond-Lamberty, B.; Wise, M. A.; Clarke, L. E.; Edmonds, J. A. RCP4.5: A Pathway for Stabilization of Radiative Forcing by 2100. *Clim. Change* **2011**, *109* (1), 77–94. https://doi.org/10.1007/s10584-011-0151-4.
(91) Riahi, K.; Rao, S.; Krey, V.; Cho, C.; Chirkov, V.; Fischer, G.; Kindermann, G.; Nakicenovic, N.; Rafaj, P. RCP 8.5-A Scenario of Comparatively High Greenhouse Gas Emissions. *Clim. Change* **2011**, *109* (1), 33–57. https://doi.org/10.1007/s10584-011-0149-y.

(92) Laruelle, G. G.; Dürr, H. H.; Lauerwald, R.; Hartmann, J.; Slomp, C. P.; Goossens, N.; Regnier, P. A. G. Global Multi-Scale Segmentation of Continental and Coastal Waters from the Watersheds to the Continental Margins. *Hydrol. Earth Syst. Sci.* **2013**, *17* (5), 2029–2051. https://doi.org/10.5194/hess-17-2029-2013.
(93) Reed, D. C.; Harrison, J. A. Linking Nutrient Loading and Oxygen in the Coastal Ocean: A New Global Scale Model. *Glob. Biogeochem. Cycles* **2016**, *30* (3), 447–459. https://doi.org/10.1002/2015GB005303.Received.
(94) Schlitzer, R. Ocean Data View odv.awi.de.
(95) Zhang, J.; Gao, Y.; Ruby Leung, L.; Luo, K.; Liu, H.; Lamarque, J. F.; Fan, J.; Yao, X.; Gao, H.; Nagashima, T. Impacts of Climate Change and Emissions on Atmospheric Oxidized Nitrogen Deposition over East Asia. *Atmos. Chem. Phys.* **2019**, *19* (2), 887–900. https://doi.org/10.5194/acp-19-887-2019.
(96) Meybeck, M.; Dürr, H. H.; Vörösmarty, C. J. Global Coastal Segmentation and Its River Catchment Contributors: A New Look at Land-Ocean Linkage. *Global Biogeochem. Cycles* **2006**, *20* (1), 1–15. https://doi.org/10.1029/2005GB002540.
(97) Boudreau, P. A Method-of-Lines Code for Carbon and Nutrient Diagenesis in Aquatic Sediments. *Comput. Geosci.* **1996**, *22* (5), 479–496.
(98) Wang, Y.; Van Cappellen, P. A Multicomponent Reactive Transport Model of Early Diagenesis: Application to Redox Cycling in Coastal Marine Sediments. *Geochim. Cosmochim. Acta* **1996**, *60* (16), 2993–3014. https://doi.org/10.1016/0016-7037(96)00140-8.
(99) Qi, J. H.; Shi, J. H.; Gao, H. W.; Sun, Z. Atmospheric Dry and Wet Deposition of Nitrogen Species and Its Implication for Primary Productivity in Coastal Region of the Yellow Sea, China. *Atmos. Environ.* **2013**, *81*, 600–608. https://doi.org/10.1016/j.atmosenv.2013.08.022.
(100) Wu, S.-P.; Dai, L.-H.; Wei, Y.; Zhu, H.; Zhang, Y.-J.; Schwab, J. J.; Yuan, C.-S. Atmospheric Ammonia Measurements along the Coastal Lines of Southeastern China: Implications for Inorganic Nitrogen Deposition to Coastal Waters. *Atmos. Environ.* **2018**, *177*, 1–11. https://doi.org/10.1016/j.atmosenv.2017.12.040.
(101) Nakamura, T.; Matsumoto, K.; Uematsu, M. Chemical Characteristics of Aerosols Transported from Asia to the East China Sea: An Evaluation of Anthropogenic Combined Nitrogen Deposition in Autumn. *Atmos. Environ.* **2005**, *39* (9), 1749–1758. https://doi.org/10.1016/j.atmosenv.2004.11.037.
(102) Lehrter, J. C.; Ko, D. S.; And, L. L. L.; Penta, B. Predicted Effects of Climate Change on Northern Gulf of Mexico Hypoxia. *Springer International Publishing AG*. 2017, pp 174–214. https://doi.org/10.1007/978-3-319-54571-4.
(103) Cabré, A.; Marinov, I.; Leung, S. Consistent Global Responses of Marine Ecosystems to Future Climate Change across the IPCC AR5 Earth System Models. *Clim. Dyn.* **2015**, *45* (5–6), 1253–1280. https://doi.org/10.1007/s00382-014-2374-3.
(104) Yu, G.; Jia, Y.; He, N.; Zhu, J.; Chen, Z.; Wang, Q.; Piao, S.; Liu, X.; He, H.; Guo, X.; Wen, Z.; Li, P.; Ding, G.; Goulding, K. Stabilization of Atmospheric Nitrogen Deposition in China over the Past Decade. *Nat. Geosci.* **2019**, *12* (6), 424–429. https://doi.org/10.1038/s41561-019-0352-4.
(105) Zheng, B.; Tong, D.; Li, M.; Liu, F.; Hong, C.; Geng, G.; Li, H.; Li, X.; Peng, L.; Qi, J.; Yan, L.; Zhang, Y.; Zhao, H.; Zheng, Y.; He, K.; Zhang, Q. Trends in China's Anthropogenic Emissions since 2010 as the Consequence of Clean Air Actions. *Atmos. Chem. Phys.* **2018**, *18* (19), 14095–14111. https://doi.org/10.5194/acp-18-14095-2018.
(106) Meire, L.; Soetaert, K. E. R.; Meysman, F. J. R. Impact of Global Change on Coastal Oxygen Dynamics and Risk of Hypoxia. *Biogeosciences* **2013**, *10* (4), 2633–2653. https://doi.org/10.5194/bg-10-2633-2013.

765 (107) Voss, M.; Bange, H. W.; Dippner, J. W.; Middelburg, J. J.; Montoya, J. P.; Ward, B. The Marine Nitrogen Cycle: Recent Discoveries, Uncertaintiesand the Potential Relevance of Climate Change. *Philos. Trans. R. Soc. B Biol. Sci.* **2013**, *368* (1621). https://doi.org/10.1098/rstb.2013.0121.

769 (108) Mississippi River/Gulf of Mexico Watershed Nutrient Task Force. *2017 Report to Congress*; 2017.